

Improving the viewing angle properties of microcavity OLEDs by using dispersive gratings

Wallace C. H. Choy* and C. Y. Ho

Department of Electrical and Electronic Engineering, University of Hong Kong, Pokfulam Road, Hong Kong, China.

*Corresponding authors: chchoy@eee.hku.hk

Abstract: The changes of emission peak wavelength and angular intensity with viewing angles have been issues for the use of microcavity OLEDs. We will investigate Distributed Bragg Gratings (DBRs) constructed from largely dispersive index materials for reducing the viewing angle dependence. A DBR stack mirror, aiming at a symmetric structure and less number of grating period for a practical fabrication, is studied to achieve a chirp-featured grating for OLEDs with blue emission peak of 450nm. For maximizing the compensation of the viewing angle dependence, the effects of dispersive index, grating structure, thickness of each layer of the grating, grating period and chirp will be comprehensively investigated. The contributions of TE and TM modes to the angular emission power will be analyzed for the grating optimization, which have not been expressed in detail. In studying the light emission of OLEDs, we will investigate the Purcell effect which is important but has not been properly considered. Our results show that with a proper design of the DBR, not only a wider viewing angle can be achieved but also the color purity of OLEDs can be improved.

©2007 Optical Society of America

OCIS codes: (230.3670) Light-emitting diodes; (250.3680) Light-emitting polymer; (050.2770) gratings.

References and links

1. A. Dodabalapur, L. J. Rothberg, and T. M. Miller, "Color variation with electroluminescent organic semiconductors in multimode resonant cavities," *Appl. Phys. Lett.* **65**, 2308-2310 (1994).
2. D. G. Lidzey, D. D. C. Bradley, S. J. Martin, and M. A. Pate, "Pixelated multicolor microcavity displays," *IEEE J. Select. Topics in Quantum Electron.* **4**, 113-118 (1998).
3. D. G. Lidzey, M. A. Pate, D. M. Whittaker, D. D. C. Bradley, M. S. Weaver, T. A. Fisher, and M. S. Skolnick, "Control of photoluminescence emission from a conjugated polymer using an optimised microcavity structure," *Chem. Phys. Lett.* **263**, 655-660 (1996).
4. F. S. Juang, L. H. Lai, C. J. Lin, and Y. J. Hsu, "Angular dependence of the sharply directed emission in organic light emitting diodes with a microcavity structure," *Jap. J. Appl. Phys.* **41**, 2787-2789 (2002).
5. K. Neyts, P. D. Visschere, D. K. Fork, and G. B. Anderson, "Semitransparent metal or distributed Bragg reflector for wide-viewing-angle organic light-emitting-diode microcavities," *J. Opt. Soc. Amer. B* **17**, 114-119 (2000).
6. N. Tessler, S. Burns, H. Becker, and R. H. Friend, "Suppressed angular color dispersion in planar microcavities," *Appl. Phys. Lett.* **70**, 556-558 (1997).
7. L. Hou, Q. Hou, Y. Peng, and Y. Cao, "All-organic flexible polymer microcavity light-emitting diodes using 3M reflective multilayer polymer mirrors," *Appl. Phys. Lett.* **87**, 243504 (2005).
8. C. He, Y. Tang, X. Zhao, H. Xu, D. Lin, H. Luo, and Z. Zhou, "Optical dispersion properties of tetragonal relaxor ferroelectric single crystals 0.65Pb(Mg1/3Nb2/3)O3-0.35PbTiO3," *Opt. Mat.* **29**, 1055-1057 (2007).
9. J. L. H. Chau, Y.M. Lin, A.K. Li, W.F. Su, K.S. Chang, S. L.C. Hsu, and T.L. Li, "Transparent high refractive index nanocomposite thin films," *Mater. Lett.* **61**, 2908-2910 (2007).
10. L. H. Smith, J. A. E. Wasey, and W. L. Barnes, "Light outcoupling efficiency of top-emitting organic light-emitting diodes," *Appl. Phys. Lett.* **84**, 2986-2988 (2004).
11. C. L. Lin, T. Y. Cho, C. H. Chang, and C. C. Wu, "Enhancing light outcoupling of organic light-emitting devices by locating emitters around the second antinode of the reflective metal electrode," *Appl. Phys. Lett.* **88**, 081114 (2006).
12. E. M. Purcell, "Spontaneous emission probabilities at radio frequencies," *Phys. Rev.* **69**, 681-684 (1946).
13. W. C. H. Choy and E. H. Li, "The applications of interdiffused quantum well in normally-on electro-absorptive Fabry-Perot reflection modulator," *IEEE J. Quantum Electron.* **33**, 382-393 (1997).

14. O. H. Crawford, "Radiation from oscillating dipoles embedded in a layered system," J. Chem. Phys. **89**, 6017-6027 (1989).
15. V. Bulovic, V. B. Khalfin, G. Gu, P. E. Burrows, D. Z. Garbuzov, and S.R. Forrest, "Weak microcavity effects in organic light-emitting devices," Phys. Rev. B **58**, 3730-3740 (1998).
16. X. W. Chen, W. C. H. Choy and S. He, "Efficient and rigorous modeling of light emission in planar multilayer organic light-emitting diodes", IEEE J. Display Technol. **3**, 110-117 (2007); K. Neyts, "Simulation of light emission from thin-film microcavities," J. Opt. Soc. Amer. A **15**, 962-970 (1998); W. Lukosz, "Theory of optical-environment-dependent spontaneous emission rates for emitters in thin layers," Phys. Rev. B **22**, 3030-3038 (1980).
17. P. A. Hobson, J. A. E. Wasey, I. Sage, and W. L. Barnes, "The role of surface plasmons in organic light emitting diodes," IEEE J. Sel. Top. Quantum Electron. **8**, 378-386 (2002).
18. R. H. Jordan, L. J. Rothberg, A. Dodabalapur, and R. E. Slusher, "Efficiency enhancement of microcavity organic light emitting diodes", Appl. Phys. Lett. **69**, 1997-1999 (1996).
19. Y. Kijima, N. Asai and S. Tamura, "A Blue Organic Light Emitting Diode," Jap. J. Appl. Phys. **38**, 5274-5277 (1999).
20. B. Deveaud, ed, *The Physics of Semiconductor Microcavities: from fundamentals to nanoscale devices*, (Wiley-VCY, 2007), Ch. 12, p.245.

1. Introduction

Microcavity structures are useful for modifying the light emission of organic light emission devices (OLEDs) [1-3]. However, typical microcavity structures will result in a large angular dependence on the emitting color [4], which causes problems for display applications. To reduce the color shift with viewing angle (V_{ang}) in microcavity devices, an extra scatter layer has been used on top of a microcavity OLED, in which a light control film is used for spatial color filtration of the emission [3]. However, the filtration will cause light blocking and absorption and thus reduces the device efficiency. Meanwhile, the structures with a metal mirror on one side of OLEDs and a semi-transparent silver mirror on the other side have been reported [5]. Since silver has absorption loss in visible region and is easily oxidized and diffused into organic layers, the effects may degrade the performance of OLEDs.

Distributed Bragg Reflector (DBR) has been actively studied for improving OLED performance. Since the materials used are typically transparent dielectrics, DBR has the advantage of low absorption loss. It has been found that poly (p-phenylenevinylene) (PPV) has dispersive refractive index which can reduce the V_{ang} issue [6, 7]. However, the wavelength (λ) region of PPV which contributes to large index dispersion also has intrinsic absorption loss. Besides, PPV is often used in the OLED structure. Due to the carrier transporting and balancing issues, there is a tradeoff in increasing the thickness of PPV for minimizing the color shift. Recently, some materials with large index dispersion have been reported [8, 9] which can be used for dispersive DBR. However, most of the attention has been paid on the high refractive index (n) for improving the light extraction [9] but not for improving the V_{ang} . In order to optimize the grating structures, the distribution of TE and TM modes on the angular emission power will be expressed for optimizing TE and TM grating reflectance, which has not been described in detail. In studying the light emission of OLEDs, we will tackle the Purcell effect which is important particularly for fluorescent organic materials and has not been properly considered recently [10, 11].

In this paper, index-dispersive DBR mirrors will be introduced to reduce the color shift with V_{ang} . The DBR structure will be designed to achieve chirp for increasing the effective cavity length and further minimizing the color shift. The effects of the material parameters of n magnitude and n dispersion, as well as the structural parameters of thickness of each layer, layer arrangement and number of period will be studied for reducing the V_{ang} dependence.

2. Theoretical formulation

In a microcavity OLED, the resonance λ_r (λ_r) of cavity modes can be described as

$$\lambda_r = 2\pi m \sum_i n_i(\lambda) L_i \cos \theta_i \quad (1)$$

where m is the mode number, L_i is the thickness of the i^{th} layer of the microcavity OLED structure. n_i is the refractive index and θ_i is the angle of the ray at the i^{th} layer. Generally λ_r

blue shifts with increasing V_{ang} . In order to reduce the change of λ_r with V_{ang} , one can counter-increase the cavity thickness with V_{ang} and increases $n_r(\lambda)$ with reducing λ . Here, both the cavity thickness and $n_r(\lambda)$ will be used to minimize the change of λ_r with V_{ang} .

Typically, SiO_2 , Si_3N_4 and TiO_2 are used to form DBR. However, their n has no obvious change with λ in visible light region. In order to improve the V_{ang} issue, a dielectric material with large n magnitude and n dispersion, and wide energy gap should be used like the recently reported $0.65\text{Pb}(\text{Mg}_{1/3}\text{Nb}_{2/3})\text{O}_3-0.35\text{PbTiO}_3$ (PMNT35%) [8] with an energy gap of 4.03eV. From the experimental results, the Sellmeier dispersion equation of n perpendicular (o) and parallel (e) to the uniaxial c -axis at room temperature are given as:

$$n_o^2 = 5.998 + \frac{0.2838}{\lambda^2 - 0.0369} + 0.0825 \cdot \lambda^2 \quad (2)$$

$$n_e^2 = 6.035 + \frac{0.2582}{\lambda^2 - 0.0455} + 0.0534 \cdot \lambda^2$$

The light emission of multilayered OLED structures is rigorously modeled through classical electromagnetic approach with an emitting layer sandwiched between two stacks of films taking into account the Purcell effect [12] which will be strengthened by Fabry Perot structures [13] of OLEDs. The nonradiative losses due to the metal electrode and other materials used in the structure as well as the effects of thick glass substrate have been fully considered, which have been ignored by others [5, 14, 15]. The vertical electric dipole (VED) and horizontal electric dipole (HED) are located in the recombination zone in the emission layer. The two stacks of films can be considered as two effective interfaces characterized by the total reflection and transmission coefficients. The total radiation power F_V and F_H for VED and HED, respectively, normalized by the radiation power of the dipole in an infinite medium ε_e , can be obtained [16]. Similarly, the normalized power U_V and U_H for VED and HED, respectively, transmitted to the outermost region (air) can also be obtained. For a randomly oriented dipole with equal probability for all directions in space, we have

$$F_R = \frac{1}{3}F_V + \frac{2}{3}F_H = \frac{1}{3}F_V^{TM} + \frac{2}{3}(F_H^{TE} + F_H^{TM}) \quad (3)$$

$$U_R = \frac{1}{3}U_V + \frac{2}{3}U_H = \frac{1}{3}U_V^{TM} + \frac{2}{3}(U_H^{TE} + U_H^{TM}) \quad (4)$$

where the superscript TE and TM denote the TE and TM modes respectively. The radiative decay rate of excitons Γ_r^m is modified to be $F \times \Gamma_r^0$ [16], where Γ_r^0 is the radiative decay rate in the infinite medium. It is considered that the non-radiative decay rate Γ_{nr} is a constant, the internal quantum efficiency η_{int}^{cav} in the microcavity becomes

$$\eta_{\text{int}}^{cav} = \Gamma_r^m / (\Gamma_r^m + \Gamma_{nr}) = F / [(F-1)\eta_{\text{int}}^0 + 1] \cdot \eta_{\text{int}}^0 \quad (5)$$

where η_{int}^0 is internal quantum efficiency (QE) of the bulk emitting material. The photon outcoupling QE $\eta_{cp}(\lambda)$ is defined as $U(\lambda)/F(\lambda)$. Due to change of internal QE in the microcavity [see Eq. (5)], the outcoupling QE should be modified as

$$\eta_{cp}^m(\lambda) = U(\lambda) / [1 + (F(\lambda) - 1)\eta_{\text{int}}^0] \quad (6)$$

where $\eta_{cp}^m(\lambda)$ is the modified outcoupling QE taking the Purcell effect into account. The angular power density $P(\alpha)$ in outermost region (air) can be expressed as

$$P(\alpha, \lambda) = \varepsilon_M k_0^2 \cos \alpha \left[\frac{1}{3}U_V^{TM} + \frac{2}{3}(U_H^{TE} + U_H^{TM}) \right] (k_0 \varepsilon_M^{1/2} \sin \alpha) / \pi \{ 1 + [(\frac{1}{3}F_V^{TM} + \frac{2}{3}(F_H^{TE} + F_H^{TM})) - 1]\eta_{\text{int}}^0 \} \quad (7),$$

by assuming ϵ_M is real where k_o is the wave number in vacuum and η_{int}^0 is the internal QE of the bulk emitting material. The above analysis on the dipole radiation is only for one λ at a fixed position. The emission characteristics of OLEDs are obtained by averaging the dipole radiation over the recombination zone and λ of interest. Thus we define an integrated out-coupling QE η and angular intensity distribution $I(\lambda)$ as,

$$\eta = \int_{\lambda_1}^{\lambda_2} \eta_{cp}^m(\lambda) P_0(\lambda) d\lambda / \int_{\lambda_1}^{\lambda_2} P_0(\lambda) d\lambda \quad (8)$$

$$I(\alpha) = \int_{\lambda_1}^{\lambda_2} P(\alpha, \lambda) d\lambda / \int_{\lambda_1}^{\lambda_2} P_0(\lambda) d\lambda \quad (9)$$

where (λ_1, λ_2) is the considered λ range and $P_0(\lambda)$ is the intrinsic emission spectrum of the emitting material. The external QE of OLED (η_{ext}) equals $\eta_{int}^0 \times \eta$. Meanwhile, from Eqs. (9) and (7), one can determine the TE and TM modes contributions to the output intensity which is important for optimizing the DBR structures and will be discussed in next section.

3. Results and discussion

The structure effects of layer thickness, layer structure and number of periods and the material effects of high n value and n dispersion of DBR will be investigated here to reduce the V_{ang} dependence of emission λ . The DBR will also be designed to achieve a suitable chirp which can further diminish the V_{ang} dependence. Besides PMNT [11], an index-dispersive polymer of TiO_2 doped polymer epoxy resin [9] will also be used for constructing DBR, since polymer LEDs (PLEDs) has gained intensive interest due to the simple fabrication process,. The refractive indices of organic materials, ITO and SiO_2 , Si_3N_4 are assumed to be 1.6, $2.06+0.005i$ and 1.5, 2.0 respectively. The complex permittivity of Ag and Al is taken from [17]. In the discussion, unless specify, the peak λ shift by changing V_{ang} from 0° to 30° ($\Delta\lambda$) is studied. It should be noted that the model has been verified and show very good agreement with the experimental result [18], although the details have not been shown here.

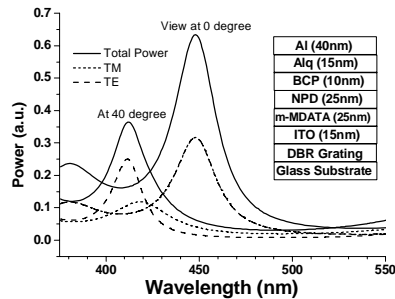


Fig. 1 The angular intensity spectrum of Al(40nm) /Alq(15nm) /BCP(10nm) /NPD(25nm) /m-MDATA(25nm) /ITO(15nm) /PMNT(70nm) / SiO_2 (20nm)] $\times 2.5$ periods. Inset is the OLED structure.

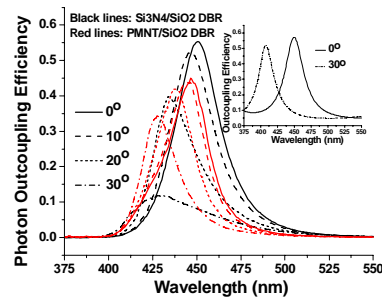


Fig. 2 The photon outcoupling QE of OLEDs with (a) [Si_3N_4 (57nm) / SiO_2 (75nm)] $\times 2.5$ periods DBR and (b) [PMNT(70nm) / SiO_2 (20nm)] $\times 2.5$ periods DBR. Inset is the outcoupling QE of (a).

In optimizing the DBR structure, one needs to determine the significance of the TE and TM reflectance of the DBR on the electroluminescent (EL) spectrum. For this reason, the contributions of TE and TM modes to the angular power distribution described by Eqs. (7) and (9) have been investigated. The device structure is Al(40nm) /Alq(15nm) /BCP(10nm) /NPD(25nm) /m-MDATA(25nm) /ITO(15nm) /PMNT(70nm) / SiO_2 (20nm)] $\times 2.5$ periods (see inset of Fig. 1). At $V_{ang}=0$, the power contributed by TE modes is the same as that of the

TM modes. It is because the reflectance spectrum of TE is the same as TM at zero degree. Therefore, the TE and TM spectra coincide to each other as shown in Fig. 1. However, when the V_{ang} increases, the power contributed by the TM modes to the peak of the total spectrum reduces (due to the decrease of TM reflectance) as compared to that of the TE modes (see Fig. 1). The features also happen in other microcavity OLED structures. As a result, the TE reflectance spectrum of DBR structures will be discussed hereby for improving the V_{ang} .

3.1 Structure effects

A blue OLED [19] of Al(40nm) /Alq(15nm) /BCP(10nm) /NPD(25nm) /m-MDATA (25nm) /ITO(15nm) / $[\text{Si}_3\text{N}_4(57\text{nm})/\text{SiO}_2(75\text{nm})]\times 2.5$ periods is investigated here. The $\frac{1}{4}\lambda$ thickness of Si_3N_4 and SiO_2 is designed to make the emission λ peaks at 450nm. As shown in A blue OLED [19] of Al(40nm) /Alq(15nm) /BCP(10nm) /NPD(25nm) /m-MDATA (25nm) /ITO(15nm) / $[\text{Si}_3\text{N}_4(57\text{nm})/\text{SiO}_2(75\text{nm})]\times 2.5$ periods is investigated here. As shown in Table 1 (column A), the peak λ blue shifts by 23.2nm to 427nm. For the target of reducing the V_{ang} dependence, Si_3N_4 is replaced by index-dispersive PMNT. Meanwhile, in order to take the full advantage of the dispersive feature and large magnitude of the n of PMNT, the thickness ratio of PMNT and SiO_2 is increased. Our results show that when thickness of SiO_2 is reduced, the stop band of the DBR reflectance spectrum decreases, which will improve the color purity due to the narrowing of the emission spectrum of NPD by the DBR as shown in Fig. 3(b) where EL of the non-cavity OLEDs is obviously broader than the OLEDs with DBR grating. However, when the thickness of SiO_2 is further reduced, most of the light will be filtered out and η_{ext} will decrease, i.e. a tradeoff between color purity and η_{ext} . Concerning PMNT, when its thickness increases, $\Delta\lambda$ reduces. However, when PMNT is too thick, the DBR reflectance spectrum will red shift too much and make the DBR not match with the emission spectrum of NPD and thus η_{ext} reduces. With the understanding of the thickness effects, the period structure of PMNT (70nm) and SiO_2 (20nm) is finalized. As shown in Table 1 (column C) and Fig. 2, by replacing the 2.5 periods of $[\text{Si}_3\text{N}_4(57\text{nm})/\text{SiO}_2(75\text{nm})]$ with 2.5 periods of $[\text{PMNT}(70\text{nm})/\text{SiO}_2(20\text{nm})]$, $\Delta\lambda$ reduces to 18.8nm and the spectrum has no significant distortion while for the $\text{Si}_3\text{N}_4(57\text{nm})/\text{SiO}_2(75\text{nm})$ DBR, the photon outcoupling QE at 30° is distorted significantly (see Fig. 2). It is because the peak outcoupling QE (without taking into account the emission spectrum of NPD) as shown in the inset of Fig. 2 is blue shifted to 406nm which is too far from the emission peak of NPD.

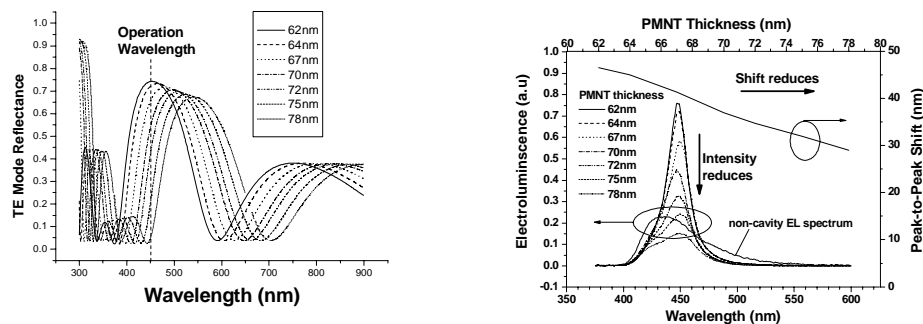


Fig. 3. (a). the TE reflectance spectrum of $[\text{PMNT}/\text{SiO}_2(20\text{nm})]\times 2.5$ periods DBR with various PMNT thicknesses. (b). EL spectrum and $\Delta\lambda$ for various PMNT thicknesses.

Table 1. $\Delta\lambda$ of DBR structures. (a) [Si₃N₄(57nm)/SiO₂(75nm)], (b) [PMNT(70nm)/SiO₂(20nm)] with a constant index $n \cong 2.6$ for PMNT, (c) same grating as (b) but with a dispersive PMNT index, and (d) polymer DBR of [TiO₂:PMMA (75nm) / PEDOT(20nm)].

	A	B	C	D
$\Delta\theta$	($\Delta\lambda$ in nm)			
10	3.8	2.6	1.9	2
20	16.3	12.8	8.8	7.5
30	23.2	20.6	18.8	16.3

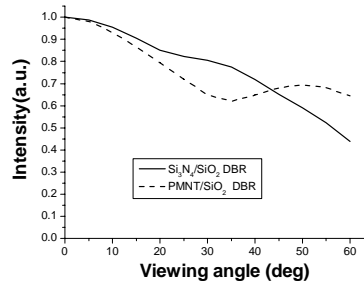


Fig. 4 The angular intensity of OLEDs with the gratings of Si₃N₄(57nm)/SiO₂(75nm) and PMNT(70nm)/SiO₂(20nm).

The DBR layer arrangement of high index (H) PMNT and low index (L) SiO₂ can be, starting from ITO, (a) HLHL...HL, (b) HLHL...HLH, (c) LHLH...LH and (d) LHLH...LHL, since the substrate is glass and it is reasonable to consider the SiO₂ layer and glass substrate have same n . Therefore, the structure of (a) is the same as (b) and (c) the same as (d). Our results show that the structure of (a) is better than (c). Take two periods DBR as an example, structure (a) will make $\Delta\lambda$ decrease 20nm when that of (b) is 27.5nm. Here, 2.5 periods of PMNT(70nm)/SiO₂(20nm) will be used as the DBR as similar periods of DBR of TiO₂(nm)/SiO₂(nm) has been experimentally used for improving the efficiency of OLEDs [18]. In case smaller $\Delta\lambda$ is needed, the number of the DBR unit period and the thickness of PMNT can be increased. For instance, by increasing the thickness of PMNT from 70nm to 145nm, $\Delta\lambda$ can be reduced from 18.8nm to 15nm. Meanwhile, DBR with asymmetric periods can be used to further reduce $\Delta\lambda$ [20].

3.2 Material effects

By comparing the typical DBR structure (column A of Table 1) and the optimized structure (column C), it can be observed that $\Delta\lambda$ is considerably reduced particularly when $V_{\text{ang}} < 20^\circ$. This is contributed by not just the structure design stated previously, but also by the material effects and chirp. When n magnitude increases from Si₃N₄ ($n \cong 2$) to PMNT ($n \cong 2.6$), $\Delta\lambda$ reduces from 23.2nm (column A) to 20.6nm (column B). This can be explained by Snell's law that due to a higher n_i value, the change of θ_i in Eq. (1) reduces for a larger change of external V_{ang} . Therefore, $\Delta\lambda$ is reduced. On the other hand, the index dispersion of PMNT, i.e. n increases when λ decreases, can compensate the reduction of $\cos\theta_i$ and further diminish $\Delta\lambda$ as can be observed from Table 1 by comparing column (B) and (C).

3.3 Chirp effects

Chirp can be introduced into the OLEDs by designing the DBR that the emission peak λ of 450nm is at the short λ side of the DBR reflectance spectrum [see Fig. 3(a)]. In this case, the effective optical path length of the microcavity OLED is increased when the emission λ is

reduced. As a result, $\Delta\lambda$ can be compensated. By increasing PMNT thickness from 62nm to 78nm, the DBR reflectance spectrum will red shift. The DBR reflectance at the emission peak λ of 450nm will change from the top to the bottom value at the short λ side of DBR [see Fig. 3(a)]. $\Delta\lambda$ will then reduce from 25nm to 15.5nm, which shows the effect of chirp on minimizing $\Delta\lambda$ as shown in Fig. 3(b). However, at the same time, the emission intensity will decrease to about 1/5 of the case of PMNT = 62nm [see Fig. 3(b)]. Taking into account the tradeoff between $\Delta\lambda$ and emission intensity, the PMNT thickness is set at 70nm. Moreover, when V_{ang} increases, the reflectance spectrum will blue shift. The increase of the effective optical path length will therefore diminish and degrade the compensation. By introducing the high n value and n dispersion of PMNT, the blue shift of the reflectance spectrum reduces and thus enhances the chirp for minimizing $\Delta\lambda$.

Figure 4 shows the angular intensity distribution of microcavity OLEDs. When $V_{\text{ang}} < 20^\circ$, the change of the intensity of the PMNT grating is slightly larger than that of the conventional DBR. The change becomes larger when the angle increases to 30° but improves when the angle further increases and better than that of the conventional DBR when the angle $> 45^\circ$. As a consequence, by changing the DBR structure from the typical the $\text{Si}_3\text{N}_4(57\text{nm})/\text{SiO}_2(75\text{nm})$ DBR to the PMNT(70nm)/ $\text{SiO}_2(20\text{nm})$ DBR, there is generally no significant degradation in the angular intensity and eventually, the change recovers and is even better than the conventional DBR when the angle is $> 45^\circ$.

While QE and lifetime of PLEDs is continuously improving, it would be interesting to study the microcavity PLED using polymer DBR. Recently, TiO_2 nanoparticles doped polymer with large n magnitude and dispersion has been reported [9]. Based on the knowledge on optimizing the PMNT grating, a 2.5 periods of TiO_2 doped polymer (75nm)/PEDOT:PSS (20nm) has been studied. Since the TiO_2 nanocomposite film dissolved in Tetrahydrofuran and PEDOT:PSS dissolved in water, it is possible to develop the polymer DBR. From column D of Table 1, $\Delta\lambda$ is further reduced to 16.3nm, which makes the polymer structure attractive for DBR applications.

4. Conclusions

The reduction of $\Delta\lambda$ by using index-dispersive DBR grating has been investigated. The expression of the TE and TM modes on the angular intensity has been detailed for optimizing the DBR structure. The light emission and QE of OLEDs has been studied with the Purcell effects. In optimizing DBR structures, material and structure parameters and chirp have been studied. Due to the dispersive feature and large magnitude of the PMNT refractive index, the $\Delta\lambda$ is reduced by ~50% at small viewing angles as compared with the typical DBR structure reported without a significant degrade in angular intensity. Our results also show that polymers with large dispersive index can have potential for making microcavity PLEDs with less V_{ang} dependence.